Title

Unenhanced MDCT in suspected urolithiasis: improved stone detection and density measurements using coronal maximum-intensity-projection images.

Journal

American Journal of Roentgenology, 201(5)

ISSN

0361-803X

Authors

Corwin, Michael T
Hsu, Margaret
McGahan, John P
et al.

Publication Date

2013-11-01

DOI

10.2214/ajr.12.10389

Peer reviewed

HHS Public Access

Author manuscript

AJR Am J Roentgenol. Author manuscript; available in PMC 2016 September 07.

Published in final edited form as:

AJR Am J Roentgenol. 2013 November ; 201(5): 1036–1040. doi:10.2214/AJR.12.10389.

Unenhanced MDCT in Suspected Urolithiasis: Improved Stone Detection and Density Measurements Using Coronal Maximum-Intensity-Projection Images

Michael T. Corwin[1], **Margaret Hsu**[1], **John P. McGahan**[1], **Machelle Wilson**[2], and **Ramit Lamba**[1]

[1]Department of Radiology, University of California, Davis Medical Center, 4860 Y St, Ste 3100, Sacramento, CA 95817.

[2]Department of Public Health Sciences, University of California, Davis, Davis, CA.

Abstract

OBJECTIVE—The purpose of this study was to determine whether coronal maximum-intensity-projection (MIP) reformations improve urinary tract stone detection and density measurements compared with routine axial and coronal images.

MATERIALS AND METHODS—Forty-five consecutive patients who underwent MDCT for suspected urolithiasis were included. Two radiologists independently determined the number of stones on 5-, 3-, and 1.25-mm axial, 5- and 3-mm coronal, and 5-mm coronal MIP images. The reference standard was obtained by consensus review using all six datasets. Stone density was determined for all calculi 4 mm or larger on all datasets.

RESULTS—There were a total of 115 stones. Reader 1 identified 111 (96.5%), 112 (97.4%), 97 (84.3%), 102 (88.7%), 99 (86.1%), and 85 (73.9%) stones and reader 2 identified 105 (91.3%), 102 (88.7%), 85 (73.9%), 89 (77.4%), 89 (77.4%), and 76 (66.1%) stones on the MIP, 1.25-mm axial, 3-mm axial, 3-mm coronal, 5-mm coronal, and 5-mm axial images, respectively. Both readers identified more stones on the MIP images than on the 3- or 5-mm axial or coronal images ($p < 0.0001$). The mean difference in stone attenuation compared with the thin axial images was significantly less for the MIP images (44.6 HU) compared with 3-mm axial (235 HU), 3-mm coronal (309 HU), and 5-mm coronal (329.6 HU) or axial images (347.8 HU) ($p < 0.0001$).

CONCLUSION—Coronal MIP reformations allow more accurate identification and density measurements of urinary tract stones compared with routine axial and coronal reformations.

Keywords

maximum intensity projection; MDCT; nephrolithiasis; renal stones; urolithiasis

Unenhanced MDCT is the current imaging modality of choice for suspected urolithiasis, with reported sensitivity of 95–98% and specificity of 96–100% [1, 2]. MDCT can reliably determine urinary tract stone size, location, and presence of urinary obstruction. In addition,

Address correspondence to M. T. Corwin (michael.corwin@ucdmc.ucdavis.edu).

stone density can be measured, which can help predict stone composition and response to therapies such as shock wave lithotripsy [1, 3–5].

The advent of MDCT with 16 or more detector rows has resulted in the routine acquisition of isotropic voxels that can be reconstructed at a section thickness of 1 mm or even less as well as multiplanar reconstructions. Thus, there has been interest in determining the slice thickness and imaging plane that enable the most accurate and efficient assessment of urinary tract stones. Thick sections of 5–10 mm have been shown to miss small stones and underestimate both size and attenuation measurements primarily due to partial volume effects [6, 7]. Slice thicknesses less than 5 mm have been shown to improve stone detection and result in more accurate attenuation measurements both in vitro and in vivo [7–9]. Additionally, coronal reformations have been shown to improve stone detection and size measurements compared with thick axial images [10, 11].

Although viewing thin axial and coronal images together may lead to improved stone detection, the review time is significantly lengthened. Not only must more images of the kidneys and collecting systems be viewed with thin slices but evaluation of the remainder of the entire abdomen and pelvis also will be lengthened. Additionally, the noise level increases as the slice thickness decreases, which may cause limitations in evaluation of other organ systems and low-contrast lesions.

Maximal-intensity-projection (MIP) techniques display the voxel with the highest attenuation value along a line (or search ray) projected through the dataset in the given volume, forming a 2D image. MIP is a widely used rendering tool for evaluation and display in CT angiography. We investigated the utility of coronal MIP reformations in detection and Hounsfield density measurement of urinary tract stones. We hypothesized that an increased conspicuity of stones on MIP images would result in improved detection of urinary tract stones compared with routine axial and coronal reformats. Furthermore, because there are no partial volume averaging effects with MIPs, density measurements may be more accurate. Therefore, the purpose of this study was to compare the accuracy of coronal MIP images with routine axial and coronal reformations in the detection and density measurement of urinary tract stones.

Materials and Methods

Study Group

This HIPAA-compliant study was approved by the institutional review board, and a waiver of informed consent was obtained because of its retrospective nature. A search of our single-institution radiology database was performed to identify all unenhanced renal stone protocol CT examinations from July 1, 2011, to October 31, 2011. The radiology reports were viewed to determine cases that were positive for nephrolithiasis and yielded 88 cases. Thirteen patients were excluded because they had more than 10 renal stones. They were eliminated because accurate and reliable stone counts were difficult to obtain in these patients due to clustering of small stones. Patients were also excluded because of the presence of ureteral stents ($n = 7$), staghorn calculi ($n = 6$), and lack of MIP images ($n = 12$). Follow-up studies after treatment of stones ($n = 5$) were not included in this study. The final study group

consisted of 45 patients (20 men and 25 women; mean age, 43 years; age range, 19–74 years).

CT Technique

All CT examinations were performed on a 64-MDCT scanner (VCT, GE Healthcare). All studies were performed using a detector configuration of 64 × 0.625, beam collimation of 40 mm, 120 kVp, pitch of 1.375, gantry rotation of 0.5 second, and variable tube current using automated dose modulation (Smart mA, GE Healthcare) with a prescribed noise index of 30 for the 1.25-mm reconstructed images. Images were reconstructed axially at a thickness and interval of 1.25 and 1.25 mm and 5 and 5 mm, respectively, using a standard body filter. Nonoverlapping isotropic 0.625-mm datasets were used to obtain coronal reformations at a thickness and interval of 5 and 3 mm and MIP reformations at a thickness and interval of 5 and 3 mm. These images constituted our routine renal stone MDCT protocol and were obtained prospectively. We then retrospectively created coronal and axial reformations each at a thickness and interval of 3 and 3 mm, for the purposes of the study. The mean volume CT dose index was 14.21 mGy, the mean dose-length product was 744.25 mGy · cm, and the mean effective dose was 12.65 mSv (using a conversion factor of 0.017) [12].

Image Analysis

Six sets of images (5-mm axial, 3-mm axial, 1.25-mm axial, 5-mm coronal, 3-mm coronal, and 5-mm coronal MIP) were independently reviewed for each patient by two board-certified radiologists who had 7 and 14 years of experience and specialized training in abdominal imaging. They were blinded to any clinical information, including the original radiology reports. Patients were randomly split into five groups. Each radiologist independently viewed only one set of images (5-mm axial, 3-mm axial, 1.25-mm axial, 5-mm coronal, 3-mm coronal, or 5-mm MIP) for each group at a time. For each group of patients, the order in which the different image sets were reviewed was varied to minimize any potential recall bias on any one image set. The radiologists were instructed to count the number of stones in each kidney and ureter (proximal, mid, distal) and the bladder for each set of images without referring to any other image set.

A third radiologist who had 2 years of experience then obtained stone densities by placing regions of interest (ROIs) over each stone 4 mm or more in greatest diameter. This size threshold was chosen to ensure that the ROIs were placed completely within the stone, without including surrounding soft tissue. This was performed for all six imaging sets. For each stone, the difference in attenuation values between the thin 1.25-mm axial images and each of the four image sets was calculated.

Reference Standard

The reference standard for the number of stones was determined using consensus review after the blinded review had been performed. The same two radiologists viewed all six image sets together. Note was made of any vascular or parenchymal calcifications or phleboliths that could have led to an error in interpretation. The reference standard for stone density was performed by placing ROIs over all stones 4 mm or larger using the 1.25-mm axial images.

Statistical Analysis

The error (difference from the consensus) in the number of stones detected for each image set was calculated. Each image set was compared by then calculating the differences in the error for each pairwise comparison and using the Statistical Analysis System (SAS) UNIVARIATE procedure (SAS Institute) to perform the Wilcoxon signed rank test. Differences between readers were tested using NPAR1WAY procedure (SAS Institute) to perform the Wilcoxon rank sum test. The difference in attenuation between thin axial images and each of the five other image sets was calculated for each stone identified. Effects due to image type were tested using a repeated measures analysis of variance with the patient as a random effect.

Results

There were a total of 115 stones. Reader 1 correctly identified 111 (96.5%), 112 (97.4%), 97 (84.3%), 102 (88.7%), 99 (86.1%), and 85 (73.9%) stones on the MIP, 1.25-mm axial, 3-mm axial, 3-mm coronal, 5-mm coronal, and 5-mm axial images, respectively. Reader 2 correctly identified 105 (91.3%), 102 (88.7%), 85 (73.9%), 89 (77.4%), 89 (77.4%), and 76 (66.1%) stones on the MIP, 1.25-mm axial, 3-mm axial, 3-mm coronal, 5-mm coronal, and 5-mm axial images, respectively. Thus, both readers identified more stones on the MIP images than on the 3- or 5-mm coronal or axial images ($p < 0.0001$). There was no significant difference in the average error from consensus between MIP and 1.25-mm axial images ($p = 1.0$). Of the four stones reader 1 missed on the MIP images, three were 1 mm or less and one was in the mid ureter, proximal to two larger obstructing distal ureteral stones. Of the 10 stones reader 2 missed on the MIP images, six were 1 mm or less, two were directly adjacent to additional stones and interpreted as a single stone instead of two separate stones, one was interpreted as a vascular calcification, and one was in the mid ureter. Reader 1 identified 2, 3, 0, 1, 3, and 1 false-positive findings on the MIP, 1.25-mm axial, 3-mm axial, 3-mm coronal, 5-mm coronal, and 5-mm axial images, respectively. The two false-positive findings of reader 1 on MIP images were a bladder wall calcification and a vascular calcification. Reader 2 identified 4, 5, and 2 false-positive findings on the MIP, 1.25-mm axial, and 3-mm axial images, respectively. All four false-positive findings of reader 2 on MIP images were single stones interpreted as two separate stones. Figures 1 and 2 show examples of improved stone visualization with MIP images compared with routine reformations.

A total of 55 stones in 14 patients were 4 mm or larger and therefore measured for Hounsfield density. The mean attenuation value was 1008 HU measured on the 1.25-mm axial images and 964, 781, 700, 661, and 679 HU for the MIP, 3-mm axial, 3-mm coronal, 5-mm coronal, and 5-mm axial images, respectively. The mean difference in attenuation per stone compared with the thin axial images was significantly less for the MIP images (44.6 HU, [SD] 99.9) compared with the 3-mm axial (234.7 HU, 142.4), 3-mm coronal (308.9 HU, 195.7), 5-mm coronal (329.6 HU, 172.2) or axial images (347.8 HU, 202.8) ($p < 0.0001$).

Discussion

Unenhanced MDCT is the first-line imaging modality for evaluation of suspected urolithiasis [13]. Acquisition of isotropic voxels is performed with MDCT using 16 or more detector rows, allowing reconstructions to be performed at slice thicknesses of 1 mm or less and in any plane. Thus, varying MDCT techniques have been studied to determine the optimal protocol for assessment of urinary tract stones. The results of our study show that coronal MIP images are superior to 5- or 3-mm axial and 3- or 5-mm coronal images in detecting and characterizing the density of urinary tract stones.

Smaller slice thickness allows improved renal stone detection and attenuation characterization, both due to reduction in volume averaging. Thicker sections of 5–10 mm have been shown to underestimate stone number, size, and attenuation measurements in vitro [6, 7]. Another in vitro study by Ketelslegers and Van Beers [8] revealed increasing stone detection and more accurate attenuation characterization with decreasing slice thickness. A study of 72 patients with urinary tract stones by Memarsadeghi et al. [14] showed improved stone detection using 3-mm axial images compared with 5-mm axial images.

Coronal images have also been studied in urinary tract stone detection. Because the urothelial system is oriented craniocaudad, this plane theoretically allows faster detection because fewer images need to be viewed. Metser et al. [10] showed 3-mm coronal reformations to improve stone detection and radiologist confidence when compared with 5-mm axial images. A study by Memarsadeghi et al. [14] showed no improved stone detection using 3-mm coronal reformats compared with 3-mm axial sections; however, evaluation time was reduced with the coronal images. Lin et al. [15] found similar stone detection using 3-mm coronal images and 2.5-mm axial images alone; however, an increased number of stones were identified using both sets of images together.

Thus, it is clear that stone detection is improved using some combination of thin (less than 5 mm) axial and coronal images. However, there are limitations of using such techniques. First, image noise increases with decreasing slice thickness. Although this should not limit evaluation of larger stones because of the inherent high contrast between the dense renal stone and the kidney or collecting system, it may result in difficulty distinguishing isolated voxels of high attenuation because of noisy datasets from punctate stones. It may also limit evaluation of the remainder of the abdomen and pelvis, particularly when a low-dose technique is used.

CT has been shown to be useful in identifying other causes of acute flank pain in the absence of urolithiasis. Therefore, optimizing the technique for detecting other abnormalities is important, particularly given the low contrast resolution because of the lack of IV contrast administration [16]. Thinner slices also lengthen evaluation time because more images must be viewed. Likewise, viewing all axial and coronal images will significantly lengthen evaluation time. Although thin images of approximately 1 mm may be accurate for stone detection and characterization, the increased noise and prolonged evaluation time limit this approach on a routine basis in our opinion. Because the urothelial system extends from the top of the kidneys to the base of the bladder, essentially the entire abdomen and pelvis would

have to be viewed using thin images to complete an evaluation for urolithiasis. Furthermore, it may be impractical and expensive to store the large amount of data associated with 1-mm images on a PACS in some radiology practices [17].

We have evaluated an alternative technique to detect urinary stones—viewing coronal MIP images. MIP images are created by displaying the highest density voxel in a given volume. Therefore, on a given image, the stone will be projected with the same brightness as the brightest voxel within the portion of the stone that is covered on that slice. This enables better detection because the contrast between the stone and surrounding tissues is greatly accentuated. This technique requires no additional radiation exposure, and the images can be automatically generated by the CT scanner without additional technologist or radiologist effort. We are aware of only one prior study that used MIP images to evaluate urinary tract stones. In this study, Van Beers et al. [18] showed improved stone detection using radiographs and MIP images together compared with radiographs alone or radiographs and 2.5-mm axial images. However, comparison with our study is difficult because details, such as the slice thickness of MIP images and number of detector rows of the CT scanner, were not reported.

Our data support the use of coronal MIP images because there was increased stone detection compared with both 3- and 5-mm axial and 3- and 5-mm coronal images. The detection rate on the MIP images of 96.5% (reader 1) and 91.3% (reader 2) in our study was similar to the detection rate of 95.2% reported by Metser et al. [10] for 3-mm coronal images. However, these percentages cannot be directly compared because our reference standard had higher sensitivity using 1.25-mm axial images in addition to the other images, whereas no images below 3 mm were used for the reference standard in that study. Therefore, it is likely that more small stones were identified on our consensus review, resulting in lower rates of stone detection for all image sets. This is supported by our lower rates of detection (88.7% and 77.4% for readers 1 and 2, respectively) on comparable 3-mm coronal images. Additionally improved reader efficiency can be expected using 5-mm MIP images compared with 3-mm or thinner axial images because fewer images need to be viewed both due to thicker slices and that the urinary tract is longer in the craniocaudal direction than anteroposterior. Importantly, stone detection in our study was as accurate using 5-mm MIP images as 1.25-mm axial images.

We have also shown that urinary tract stone attenuation values are more accurately measured on MIP images. This is due to the lack volume averaging and identification of the highest density voxels in the stone. The higher average attenuation supports the increased stone to surrounding tissue contrast and subsequently improved detection. Accurate attenuation values are also important for stone management. There is a correlation between stone density measured by CT and stone composition. Calcium stones have attenuation greater than 1000 HU, uric acid stones are typically less than 450 HU, and cystine stones range from 600 to 1100 HU [1, 19]. Although there is much overlap between different stone types and stones can be of mixed composition, uric acid stones can be confidently diagnosed with attenuation values less than 400 HU. This is important because these stones respond to oral dissolution therapy. Aside from oral therapy, shock wave lithotripsy (SWL) is the least invasive form of treatment of urinary tract stones. An attenuation value below 900–1000 HU

is a predictor of successful SWL, with increased failure seen in stones of higher attenuation [3–5]. Thus, accurate attenuation values are important in guiding therapy for urinary tract stones, and it has been suggested that stone density be reported in all CT cases of urolithiasis [1, 2]. In our study, the MIP images provided the closest measure of stone density compared with the thin 1.25-mm images, although a mean difference of 44.6 HU lower was seen. However, the attenuation values that guide management are broad ranges and, for example, the difference between 1500 and 1450 HU will not affect management. In cases in which the attenuation values on MIP images are close to a clinical cutoff (e.g., 1000 HU), additional measurement can be made on thin section images if available.

A limitation of the MIP technique seen in this study is the slightly worse differentiation of two or more small adjacent stones from one larger stone. This was the cause of two false-negative and four false-positive results for reader 2. Therefore, in cases in which clusters of stones are seen, reference to the coronal or thin axial images may help with this distinction. It must also be emphasized that for review of soft-tissue structures in the abdomen, the MIP images should not be used. Thus, we use coronal MIP images as the initial and most often sole technique for detection and density measurement of urinary tract stones. In the rare case in which the findings are in question on the basis of the MIP images, we also use thin 1.25-mm axial images to help clarify the results. We then use 5-mm axial and coronal images to evaluate the remainder of the abdomen and pelvis.

The main limitation of this study is the lack of an absolute standard of reference. However, CT itself is now the reference standard for renal stone detection, and we believe that the combination of thin 1.25-mm axial images, coronal MIP, 3- and 5-mm coronal, and 3- and 5-mm axial images viewed in consensus by two reviewers has high enough accuracy to serve as the reference standard. It is also possible that in a few instances bright pixels due to noise could have resulted in false-positive findings even on consensus review.

In conclusion, coronal MIP reformations allow more accurate detection and density measurement of urinary tract stones compared with routine axial and coronal reformations. We suggest that coronal MIP images be used as the primary technique for detection and density measurement of urinary tract stones, with conventional axial and coronal reformations available for evaluation of the remainder of the abdomen and pelvis.

Acknowledgments

Supported by the National Center for Advancing Translational Sciences, National Institutes of Health, through grant #UL1 TR000002.

References

1. Kambadakone AR, Eisner BH, Catalano OA, Sahani DV. New and evolving concepts in the imaging and management of urolithiasis: urologists' perspective. RadioGraphics. 2010; 30:603–623. [PubMed: 20462984]
2. Eisner BH, McQuaid JW, Hyams E, Matlaga BR. Nephrolithiasis: what surgeons need to know. AJR. 2011; 196:1274–1278. [PubMed: 21606289]
3. Perks AE, Schuler TD, Lee J, et al. Stone attenuation and skin-to-stone distance on computed tomography predicts for stone fragmentation by shock wave lithotripsy. Urology. 2008; 72:765–769. [PubMed: 18674803]

4. McAdams S, Kim N, Dajusta D, et al. Preoperative stone attenuation value predicts success after shock wave lithotripsy in children. J Urol. 2010; 184:1804–1809. [PubMed: 20728112]
5. El-Nahas AR, El-Assmy AM, Mansour O, Sheir KZ. A prospective multivariate analysis of factors predicting stone disintegration by extracorporeal shock wave lithotripsy: the value of high-resolution noncontrast computed tomography. Eur Urol. 2007; 51:1688–1693. discussion, 1693–1694. [PubMed: 17161522]
6. Saw KC, McAteer JA, Monga AG, Chua GT, Lingeman JE, Williams JC Jr. Helical CT of urinary calculi: effect of stone composition, stone size, and scan collimation. AJR. 2000; 175:329–332. [PubMed: 10915668]
7. Dobbins JM, Novelline R, Rhea J, Rao PM, Prien EL, Dretler SP. Helical computed tomography of urinary tract stones: accuracy and diagnostic value of stone size and density measurements. Emerg Radiol. 1997; 4:303–308.
8. Ketelslegers E, Van Beers BE. Urinary calculi: improved detection and characterization with thin-slice multidetector CT. Eur Radiol. 2006; 16:161–165. [PubMed: 15959786]
9. Memarsadeghi M, Heinz-Peer G, Helbich TH, et al. Unenhanced multi-detector row CT in patients suspected of having urinary stone disease: effect of section width on diagnosis. Radiology. 2005; 235:530–536. [PubMed: 15758192]
10. Metser U, Ghai S, Ong YY, Lockwood G, Radomski SB. Assessment of urinary tract calculi with 64-MDCT: the axial versus coronal plane. AJR. 2009; 192:1509–1513. [PubMed: 19457812]
11. Nadler RB, Stern JA, Kimm S, Hoff F, Rademaker AW. Coronal imaging to assess urinary tract stone size. J Urol. 2004; 172:962–964. [PubMed: 15311009]
12. Bongartz, G.; Golding, SJ.; Jurik, AG., et al. [Accessed June 27, 2013] European guidelines for multislice computed tomography. European Commission website. biophysics-site.com/html/msct_quality_criteria_2004.html. Published March 2004
13. Fritzsche P, Amis ES Jr, Bigongiari LR, et al. Acute onset flank pain: suspicion of stone disease—American College of Radiology ACR appropriateness criteria. Radiology. 2000; 215(suppl):683–686. [PubMed: 11037484]
14. Memarsadeghi M, Schaefer-Prokop C, Prokop M, et al. Unenhanced MDCT in patients with suspected urinary stone disease: do coronal reformations improve diagnostic performance? AJR. 2007; 189:W60–W64. [web]. [PubMed: 17646439]
15. Lin WC, Uppot RN, Li CS, Hahn PF, Sahani DV. Value of automated coronal reformations from 64-section multidetector row computerized tomography in the diagnosis of urinary stone disease. J Urol. 2007; 178:907–911. discussion, 911. [PubMed: 17651761]
16. Dalrymple NC, Verga M, Anderson KR, et al. The value of unenhanced helical computerized tomography in the management of acute flank pain. J Urol. 1998; 159:735–740. [PubMed: 9474137]
17. Yoshinobu T, Abe K, Sasaki Y, et al. Data management solution for large-volume computed tomography in an existing picture archiving and communication system (PACS). J Digit Imaging. 2011; 24:107–113. [PubMed: 19908094]
18. Van Beers BE, Dechambre S, Hulcelle P, Materne R, Jamart J. Value of multislice helical CT scans and maximum-intensity-projection images to improve detection of ureteral stones at abdominal radiography. AJR. 2001; 177:1117–1121. [PubMed: 11641185]
19. Sheir KZ, Mansour O, Madbouly K, Elsobky E, Abdel-Khalek M. Determination of the chemical composition of urinary calculi by noncontrast spiral computerized tomography. Urol Res. 2005; 33:99–104. [PubMed: 15645229]

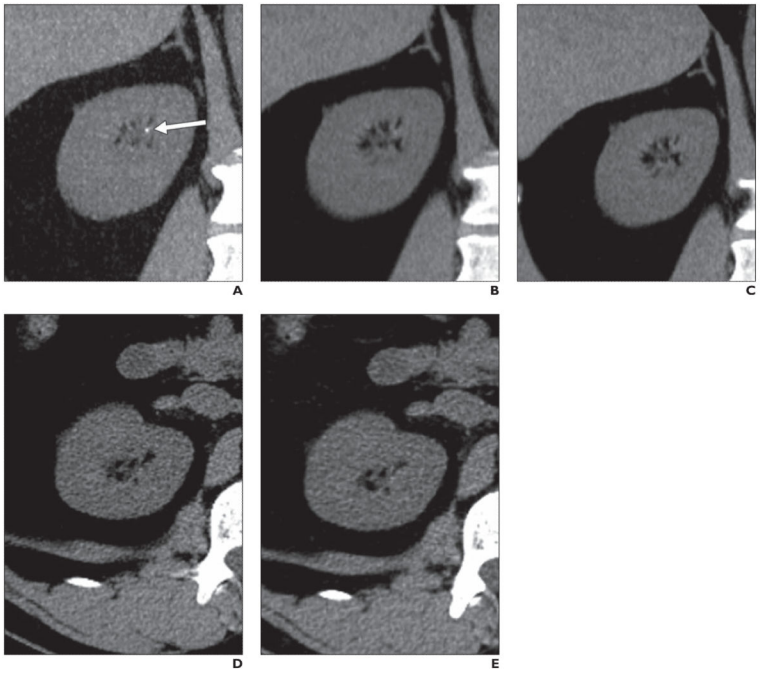

Fig. 1.

35-year-old man with right upper pole renal stone.

A–E, On 5-mm coronal maximum-intensity-projection (MIP) image (**A**), 2-mm stone (*arrow*) is seen in upper pole of right kidney. Stone is not well depicted on 5-mm coronal (**B**), 3-mm coronal (**C**), 5-mm axial (**D**), or 3-mm axial (**E**) images. Both reviewers identified stone on MIP images but not on other image sets.

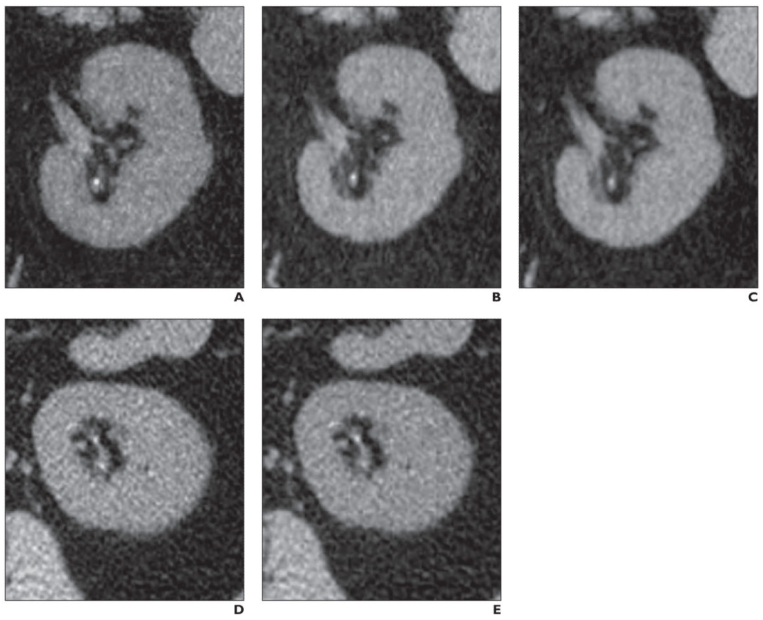

Fig. 2.

42-year-old woman with left lower pole renal stone.

A–E, On 5-mm coronal maximum-intensity-projection (MIP) image (**A**), 3-mm stone is seen in lower pole of right kidney. Stone is less well depicted on 3-mm coronal (**B**) and only faintly visualized on 5-mm coronal (**C**), 5-mm axial (**D**), and 3-mm axial (**E**) images. Reader 1 identified stone on MIP and 3-mm axial images only, and reader 2 identified stone on MIP images only.